J Electroceram (2008) 21:752–756
DOI 10.1007/s10832-007-9295-z

The incorporation of SiO_2 nanoparticles in poly(*p*-phenylenevinylene)(PPV) for PPV/SiO_2 nanocomposite

Sook Yoon · Ki Hyun Yoon · Hyung-Ho Park

Published online: 21 August 2007

Abstract The changes in surface morphology and current-voltage characteristics of poly(*p*-phenylenevinylene)(PPV) thin film has been studied by varying the amount of incorporated SiO_2 nanoparticles. The electronic structure of carbon atom in PPV and PPV/SiO_2 nanocomposite films was studied by using near-edge X-ray absorption fine structure. The surface morphology of PPV/SiO_2 nanocomposite film was found to be greatly dependent on the amount of incorporated SiO_2 nanoparticles. The current–voltage behavior of PPV/SiO_2 nanocomposite film was mainly dependent on the surface morphology of the film. The excess content of SiO_2 nanoparticles in PPV/SiO_2 nanocomposite film was revealed to induce an agglomeration of SiO_2 nanoparticles where blocking of electronic conduction happens.

Keywords SiO_2 nanoparticles · PPV · PPV/SiO_2 nanocomposite · Morphology effect

1 Introduction

Conjugated polymers have attracted much interest in applied science and technology for various possible application in the light emitting diodes (LEDs) and molecular electronic devices as a result of both easy processing and mechanical flexibility [1, 2]. However the mechanism for the current enhancement in polymer LEDs has not been yet completely understood. More recently, polymer/nanoparticles composite has been increasingly studied because of its enhanced optical and electronic properties [3–7]. For examples, incorporation of CdSe nanoparticles into conjugated polymer such as poly[2-methoxy-5-(2′-ethyl-hexyloxy)-1,4-phenylenevinylene] (MEH–PPV) showed an improvement in electrical property [8, 9]. Although this improvement was obtained with conjugated polymer/nanoparticles composite, understanding about the exact role of nanoparticle on the performance of OLEDs is far from complete and remains unclear. Further development of polymer based electronic devices requires a better understanding of such properties as the efficiency of light emission and associated mechanism. The efficiency of these devices has been found to be highly dependent on the injection behaviors of the contacts, limited primarily by the electron injection efficiency of the cathode. Accordingly, substantial improvement in electron injection efficiency therefore requires a depth study of film surfaces, including the morphology and chemical reactions of interfaces.

In this study, the incorporation of SiO_2 nanoparticles into PPV was carried out to investigate the effects on the carrier injection by observing surface chemical state and morphology of the films. Concerning about the polymer/nanoparticle composite, it was reported that optical property could be tuned by controlling the amount of SiO_2 nanoparticles in the polymer [10].

2 Experimental procedure

Poly(*p*-phenylenevinylene) was prepared via sulphonium precursor route. The starting materials of monomer were α,α′-dichloro-*p*-xylene and tetrahydrothiophene. The monomer was polymerized using equal molar quantity of NaOH. The reaction was terminated by adding an excess amount of dilute HCl to neutralize unreacted NaOH. The

S. Yoon · K. H. Yoon · H.-H. Park (✉)
Department of Ceramic Engineering, Yonsei University,
134 Shinchon-Dong, Seodaemun-Ku,
Seoul 120-749, South Korea
e-mail: hhpark@yonsei.ac.kr

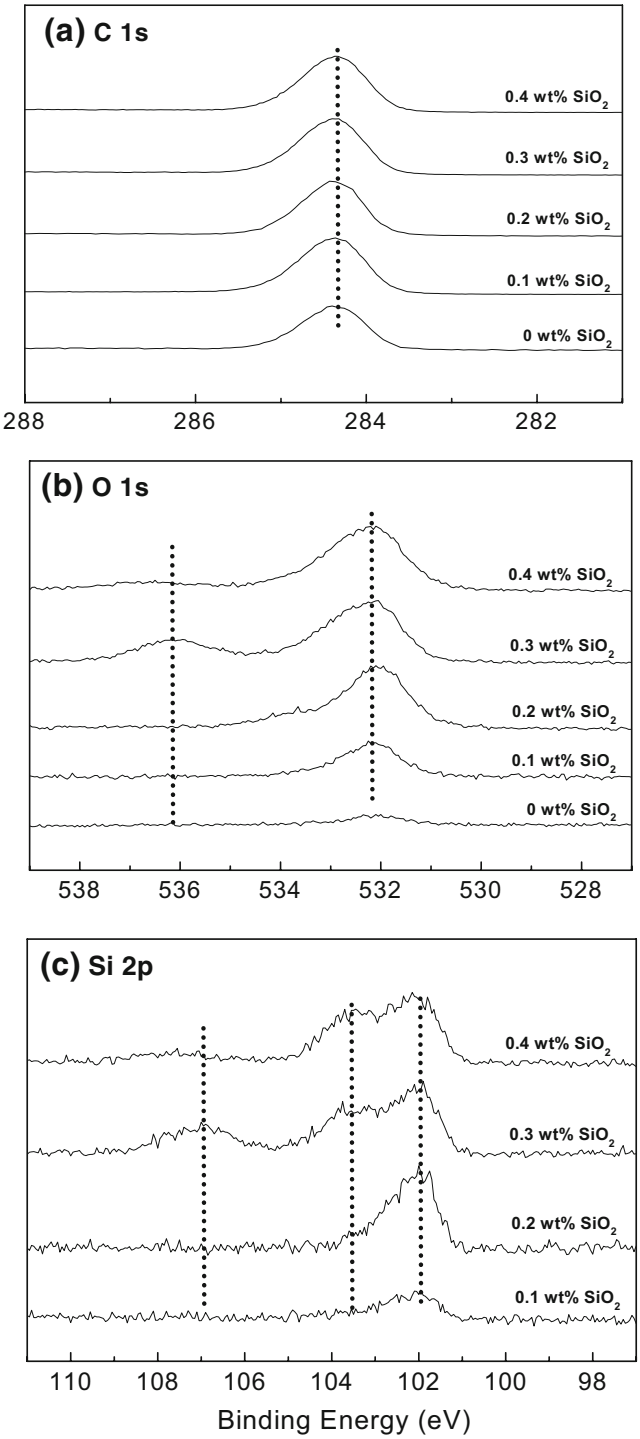

Fig. 1 (**a**) C 1s, (**b**) O 1s, and (**c**) Si 2p XPS core-level spectra with increasing SiO_2 nanoparticle content in PPV/SiO_2 nanocomposite

product was then purified by dialysis using cellulose tube. PPV film was spin coated onto clean ITO coated glass substrate, and then converted by thermal conversion under vacuum at 200°C for 4 h. The PPV/SiO_2 nanocomposite solution (0.1, 0.2, 0.3, 0.4 wt%: SiO_2 nanoparticle concentration for PPV precursor) was prepared by mixing

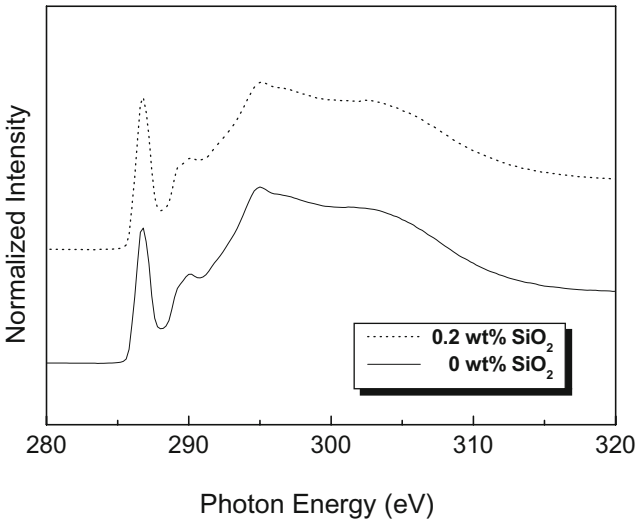

Fig. 2 Carbon K-edge NEXAFS spectra of PPV and 0.2 wt% nanocomposite films

SiO_2 nanoparticles and PPV precursor. The size of SiO_2 nanoparticle was 7 nm in diameter. PPV/SiO_2 nanocomposite film was prepared by spin-coating as the same way as for the PPV. During the preparation and transferring of sample, an exposure of sample to both oxygen and light was prevented in order to avoid photo-oxidation of the polymer. For surface chemical bonding state analysis of the films, X-ray photoelectron spectroscopy (XPS, VG Scientific, ESCALAB 220i-XL) was used with an Al Kα monochromatic source. Near-edge X-ray absorption fine structure (NEXAFS) experiments were carried out at the electron storage ring Pohang using the high-energy SGM

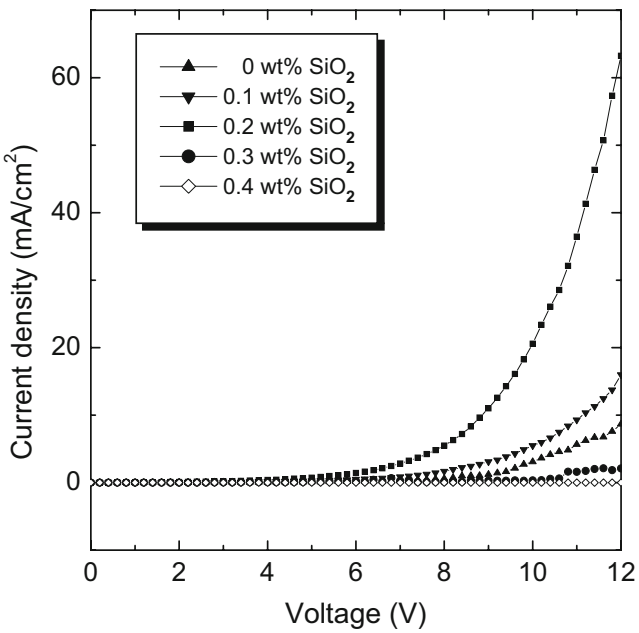

Fig. 3 Current–voltage curves for PPV and nanocomposite films

beam line. Atomic force microscopy (AFM, DI Dimension 3100) was used to monitor the surface morphology of films. For the current–voltage (I–V) measurement, three-layer devices were prepared consisting of indium–tin–oxide (ITO) coated glass substrate, polymer or polymer nanocomposite film, and 2,500 Å thick silver deposited by evaporation.

3 Results and discussion

XPS data for C 1s, O 1s, and Si 2p core levels were collected to reveal the evolution of film composition and bonding state with the increasing concentration of SiO_2 nanoparticles and were given in Fig. 1. The composition change with the incorporation of SiO_2 nanoparticles could be found by monitoring of Si content in the film. However due to the coverage with PPV polymer in the composite, the values of Si content were small but gradually changed from 1.1 to 4.1 at.%. Figure 1(a) shows C 1s core levels and 0 wt% corresponds to pure PPV without SiO_2 nanoparticle. C 1s spectra of the films show a major peak component associated with C–C/H(C bonds mainly with C but also with H) species at 284.4 eV of binding energy. A slight asymmetric broadening was found at higher binding energy side of the peaks and this was due to the contribution of C–O bonds in the polymer [11]. There was no significant change in the peak shape and peak position with the presence of SiO_2 nanoparticles. O 1s spectra are given in Fig. 1(b). O 1s peak contains C–O–C, Si–O–Si, and Si–O–H bonds. The presence of Si–O–H bonds could be confirmed in the Si 2p spectra as given in Fig. 1(c). Without SiO_2 nanoparticles, only the presence of C–O–C bonds was found at 532.1 eV. O 1s peaks showed the same behavior as C 1s with SiO_2 nanoparticles. Due to slight higher binding energy of O 1s in Si–O–Si and Si–

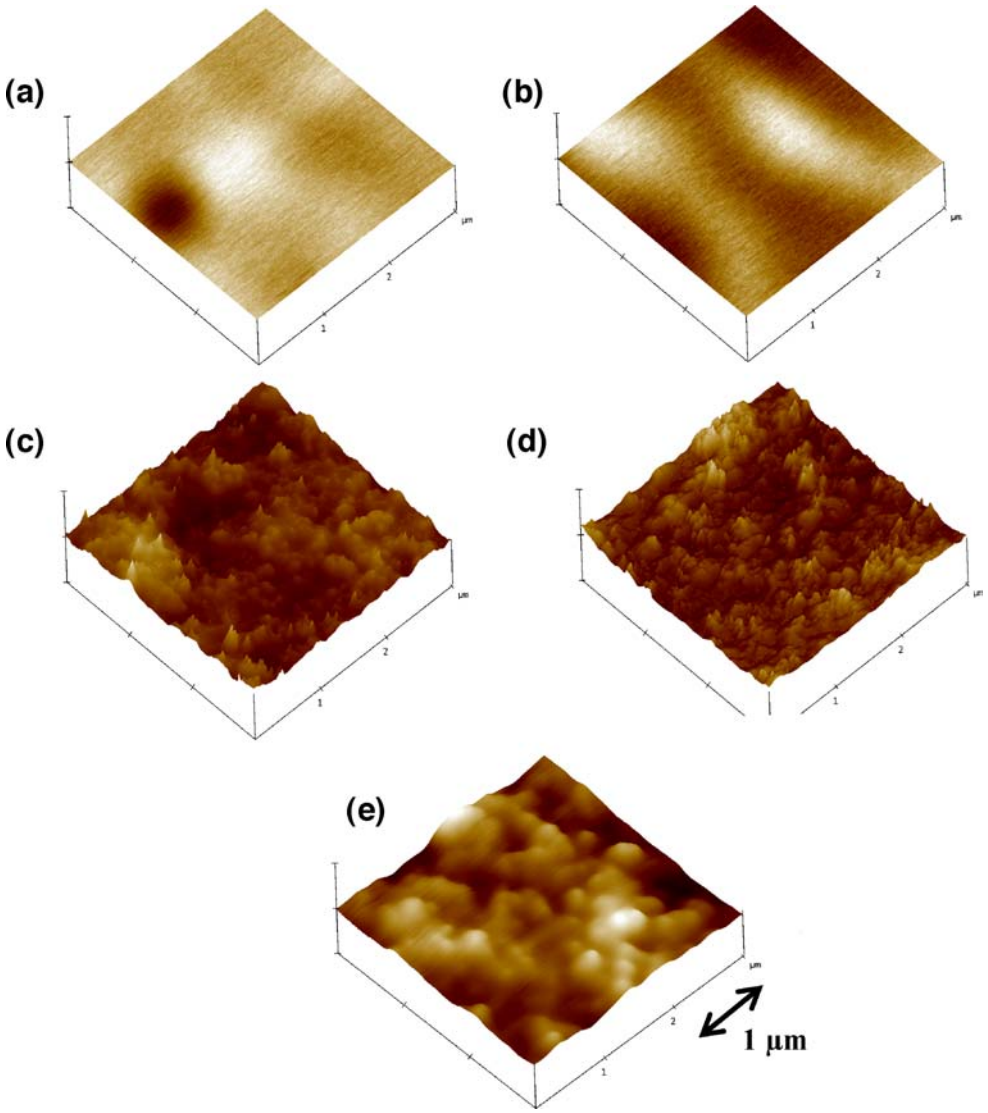

Fig. 4 AFM 3D images of (**a**) 0 wt% (pure PPV), (**b**) 0.1 wt%, (**c**) 0.2 wt%, (**d**) 0.3 wt%, and (**e**) 0.4 wt% nanocomposite films

O–H bonds than C–O–C bonds, an asymmetric broadening of O 1s peak at higher binding energy side was observed with the incorporation of SiO_2 nanoparticles. However an abnormal presence of a peak around 107 eV of binding energy was found in the case of 0.3 and 0.4 wt% PPV/SiO_2 nanocomposite films but any photoelectron or Auger electron lines of the observed element in this experiment were not matched. Furthermore any possible combination of present element with oxygen atom could not produce such a great amount of chemical shift in O 1s. This abnormal presence of O 1s peak could be originated from partial charging of local area on the film due to the incorporation of large amount of SiO_2 nanoparticles and their agglomeration [12]. This was also confirmed by Si 2p spectra shown in Fig. 1(c). Si 2p spectra showed Si–OH bonding state at around 102 eV and Si–O of SiO_2 at 103.5 eV [13]. The presence of Si–OH was induced from the hydrolysis reaction between SiO_2 nanoparticles and water in the solution precursor of PPV. The peak constitution of Si–O bonds increased with the increasing wt% of SiO_2 nanoparticles due to the limited amount of water in the solution. In Si 2p spectra, it was also possible to find an abnormal peak contribution at 107 eV of binding energy due to the localized partial charging. Through the above XPS analyses, there was no evidence for the interaction between PPV and SiO_2 nanoparticles.

The near-edge absorption spectra were acquired at the carbon K-edge of pristine PPV and 0.2 wt% PPV/SiO_2 nanocomposite films whether chemical interaction exists between PPV and SiO_2 nanoparticles or not. In Fig. 2, carbon K-edge NEXAFS spectra are given and two films showed almost same shape. The comparison of NEXAFS data between PPV and PPV/SiO_2 nanocomposite films illustrates that the incorporation of SiO_2 nanoparticle into PPV precursor does not cause a disruption of PPV conjugation, i.e., chemical interaction.

Figure 3 illustrates I–V characteristics of devices with PPV and PPV/SiO_2 nanocomposite films. The enhanced I–V characteristics in nanocomposite films with 0.1 and 0.2 wt% of SiO_2 nanoparticles were observed but degradation was found with the case of 0.3 and 0.4 wt%. For the explanation of this phenomena, AFM images were taken at 3×3 μm to demonstrate the variation of morphology with increasing SiO_2 nanoparticle content and shown in Fig. 4. The value of rms roughness tends to increase to 0.2 wt% of SiO_2 nanoparticle content but with 0.3 and 0.4 wt%, the values decrease, for example, 15, 19, 311, 222, and 243 Å with 0, 0.1, 0.2, 0.3, and 0.4 wt% of SiO_2 nanoparticle contents, respectively. The variation in the surface roughness can induce the difference in the contact area at the interface with electrode film and the effective thickness of the PPV/SiO_2 nanocomposite films. In other words, the rougher surface of 0.2 wt% PPV/SiO_2 nanocomposite causes the lager contact area and thinner effective thickness than PPV and other compositional PPV/SiO_2 nanocomposite films. So that, with the same electric filed, more current flow and higher effective field strength are possible in PPV/SiO_2 nanocomposite than in PPV and other nanocomposite films. The decreases in the rms roughness of 0.3 and 0.4 wt% of SiO_2 nanocomposite films could be explained that because of large amount of SiO_2 nanoparticles they could behave as matrix material. Then even with the increased SiO_2 nanoparticles agglomeration, the values of rms roughness was decreased [14]. The decreased conduction behavior with the case of 0.3 and 0.4 wt% could be addressed to the reduced surface roughness, i.e., reduced effective surface area and increased effective film thickness, and local agglomeration of SiO_2 nanoparticles induced local charging as shown in XPS spectra of Fig. 1.

4 Conclusions

Focusing on PPV and PPV/SiO_2 nano composite surfaces, we have demonstrated that the incorporation of SiO_2 nanoparticles has an influence on current characteristics. NEXAFS illustrates that there is no significant difference in the electronic structure between PPV and PPV/SiO_2 nanocomposite. The enhanced conductivity with the introduction of SiO_2 nanoparticles was explained with the increased effective surface area and decreased effective film thickness. The formation of PPV/SiO_2 nanocomposite induced the great variation of surface morphology and this was revealed to be the main reason of the conductivity change including the effect of local blocking of electronic conduction due to the agglomeration of the nanoparticles when introducing excess SiO_2 nanoparticles.

Acknowledgement The authors acknowledge the support from 'The National Program for 0.1 Terabit NVM Device'.

References

1. D.S. Kumar, K. Nakamura, S. Nishiyama, S. Ishii, H. Noguchi, K. Kashiwagi, Y. Yoshida, J. Appl. Phys. **93**, 2705 (2003)
2. J.H. Burroughes, D.D.C. Bradley, A.R. Brown, R.N. Marks, K. Mackay, R.H. Friend, P.L. Burns, A.B. Holmes, Nature **347**, 539 (1990)

3. P.W.M. Blom, H.F. Schoo, M. Matters, Appl. Phys. Lett. **73**, 3914 (1998)
4. A.C. Arango, S.A. Carter, Appl. Phys. Lett. **74**, 1698 (1999)
5. C.Y. Kwong, W.C.H. Choy, A.B. Djurisic, P.C. Chui, K.W. Cheng, W.K. Chan, Nanotechnology. **15**, 1156 (2004)
6. A. Kiesow, S. Strohkark, K. Löschner, A. Heilmann, A. Podlipensky, A. Abdolvand, G. Seifert, Appl. Phys. Lett. **86**, 153111 (2005)
7. R. Shenhar, T.B. Norsten, V.M. Rotello, Adv. Mater. **17**, 657 (2005)
8. G. Yu, J. Gao, J. C. Hummelen, F. Wudl, A.J. Heeger, Science. **270**, 1789 (1995)
9. L.H. Tjeng, M.B.J. Meinders, J. van Elp, J. Ghijsen, G.A. Sawatzky, Phys. Rev. **41**, 3190 (1990)
10. P.K.H. Ho, N. Tessler, R.H. Friend, Synth. Met. **102**, 1020 (1999)
11. S. Yoon, H.-J. Choi, J.-K. Yang, H.-H. Park, Appl. Surf. Sci. **237**, 450 (2004)
12. T. Gross, M. Ramm, H. Sonntag, W. Unger, H. M. Weijers, E. H. Adem, Surf. Interface Anal. **18**, 59 (1992)
13. J.-K. Hong, M.-H. Jo, D.-J. Kim, H.-H. Park, S.-H. Hyun, J. Kor. Cer. Soc. **33**, 1339 (1996)
14. C. Lu, Z. Cui, Y. Wang, Z. Li, C. Guan, B. Yang, J. Shen, J. Mater. Chem. **13**, 2189 (2003)